View metadata, citation and similar papers at core.ac.uk

brought to you by CORE

provided by ASU Digital Repository

Experimental Investigation of

Laser-Induced Optoacoustic Wave Propagation for Damage Detection

by

Venkateshwaran Ravi Narayanan

A Thesis Presented in Partial Fulfillment
of the Requirements for the Degree
Master of Science

Approved July 2019 by the
Graduate Supervisory Committee:

Yongming Liu, Chair
Houlong Zhuang
Qiong Nian

ARIZONA STATE UNIVERSITY

August 2019

ABSTRACT

This thesis intends to cover the experimental investigation of the propagation of laser-generated optoacoustic waves in structural materials and how they can be utilized for damage detection. Firstly, a system for scanning a rectangular patch on the sample is designed. This is achieved with the help of xy stages which are connected to the laser head and allow it to move on a plane. Next, a parametric study was designed to determine the optimum testing parameters of the laser. The parameters so selected were then used in a series of tests which helped in discerning how the Ultrasound Waves behave when damage is induced in the sample (in the form of addition of masses). The first test was of increasing the mases in the sample. The second test was a scan of a rectangular area of the sample with and without damage to find the effect of the added masses. Finally, the data collected in such a manner is processed with the help of the Hilbert-Huang transform to determine the time of arrival. The major benefits from this study are the fact that this is a Non-Destructive imaging technique and thus can be used as a new method for detection of defects and is fairly cheap as well.

ACKNOWLEDGMENTS

I would like to acknowledge Dr. Liu for helping me in progressing through my research work on this thesis and for teaching my many things along the way.

My fellow lab members who helped through the various stages of this work.

My family for being there for me emotionally.

TABLE OF CONTENTS

Page

LIST OF TABLES

Table Page

LIST OF FIGURES

CHAPTER 1

INTRODUCTION

Defects of different kind exist in all the materials around us. They vary from being easily discernible by visual inspection, (outer cracks, scratched surfaces etc.) to micro defects like voids which require special techniques for detecting them. There are different methods to determine the extent of these defects and they vary depending on the application of the material. Depending on the situation, the traditional nondestructive testing methods might not be feasible. For instance, if the situation calls for determining defects in aircrafts, ships, heavy machinery, etc. attaching sensors for testing might not be feasible due to regulations, cost, type of defect etc.

A good solution for such concerns might be found in non-contact nondestructive evaluation (NDE) methods. Damage detection due to propagation of Laser induced Lamb waves is such a method which is feasible and is something which is well documented. This project tries to develop a novel NDE method for using the Lamb waves induced by a Pulsed Laser. The laser is used to generate the Lamb waves in a raster scan pattern and said waves are detected by piezoelectric sensors and then processed.

1.1 Background of wave based NDE methods

Wave based nondestructive evaluation methods are of several types. Some of the most commonly used ones are where sensors are glued/attached to the surface of the sample for generation of and receiving the wave signal [1]. This method is generally not feasible for large machines are aircrafts as it would involve the usage of a large network of sensors for damage detection which would be complex to implement as well as would have the

drawback being inefficient cost wise. Traditionally, this method involves gluing the necessary sensors on the sample [2] which might cause damage on its own which further adds to the drawback of this method. A second method involves sensor actuators at the excitation terminal (such as a piezoelectric transducer) but laser based receiver terminal (such as a laser vibrometer). The excitation terminal can be replaced with a laser terminal as well making the entire process entirely non-contact based [5]. In this method, the laser causes localized heating due to being incident on the sample. Since the material surrounding the one incident spot is cooler, the material is not able to expand which causes a stress wave being generated. This ultrasonic wave would then be detected by the laser vibrometer and then the data can be processed.

Laser induced ultrasound is a concept which has been used for developing multiple testing techniques such as in nuclear power plants [6], thermographic surface breakouts [8] and more.

1.2 Motivation and Objective

This work thus intends to develop a novel method for utilizing the concept behind Laser induced ultrasound to develop a testing method for plate like samples. This is achieved by firing a MOPA laser on the sample which generates Lamb waves which are then in turn detected with the help of Piezoelectric sensors. The data from the sensors is read with the help of an Oscilloscope and stored in a flash drive. The data is then processed and is used to detect the area where damage would be present.

1.3 Major Tasks

The major undertaking of this project was three-fold. The first was development of a method for detection and then processing of the laser induced Ultrasound. The ultrasound waves are detected with the help of piezoelectric sensors which are glued on the top of sample. The second was the development of a method for a scanner system so that the laser can move on the surface of the samples. For achieving this, ASI stages were used so that a raster scanning of the surface of the sample could be performed. The last and final step was development of a technique for processing the data. This was achieved by first filtering the data and then using Hilbert-Huang Transform [3] for helping in determining a speed map to visualize the damage.

CHAPTER 2

EXPERIMENTAL SETUP

The Experimental setup for this project involved multiple devices like an oscilloscope, a function generator, a laser system, scanning system for the movement of the laser, etc. The apparatus involved and their details have been listed in table 2.1.

S No.	Name of Equipment	Model Name
1	Laser Machine	Ytterbium Pulsed Fiber Laser by IPG
2	Oscilloscope	DPO 2024 by Tektronix
3	Function Generator	SDG 1025 by Siglent
4	XY Stage	LX -4000 by ASI
5	Computer	Dell Workstation

Figure 1 represents how the various components are connected as well as the flow of data in the experimental setup.

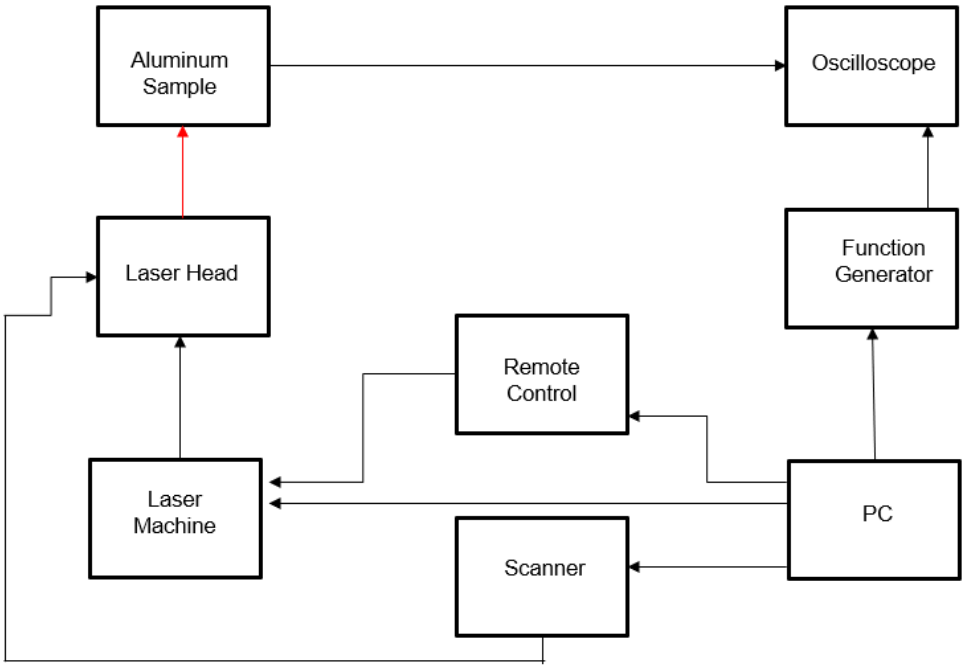

Figure 1 - Shows how the various components are connected

2.1 Principle of Laser Scanning

The laser system works after it is given commands from the computer. The laser parameters are first set with either the help of an application provided by the manufacturer or by giving commands to the laser with the help of Serial port commands. The function generator then fires a square wave to the laser machine to synchronize and fire the laser. The square wave from the function generator is displayed on the oscilloscope along with the laser signal. The data thus collected with the oscilloscope is then processed do determine the time of arrival.

For testing, the function generator's signal was set at 1000 Hz, 50% Duty and the laser parameters were set with the help of the parametric test performed. The parameters which effected the test most were the Power, the Pulse Duration (PD) and the Pulse Repetition

Rate (PRR). The parameters were set as 90% Power, 200 ns PD and 60 kHz PRR for test 2.2.2 and 20 kHz for the other tests.

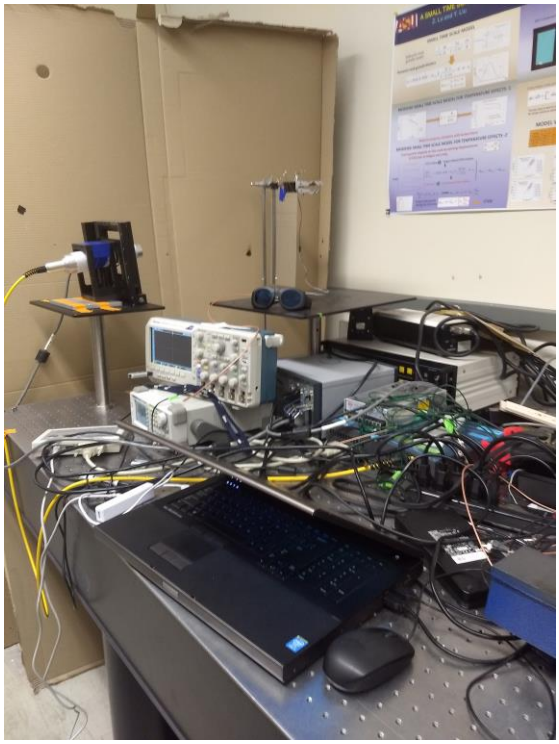

Figure 2- Experimental Setup

The experimental environment is setup in such a fashion so that the laser can be moved on the surface of a desired sample with the help of a computer so as to perform a raster scan of the surface of the sample. For this, the sample is clamped at a fixed distance from the laser head (500 mm). A scanner system was then designed so that the laser can move on the surface of the sample. The scanner system involves a LX – 4000 ASI stage and its own power supply.

2.2 Tests Conducted

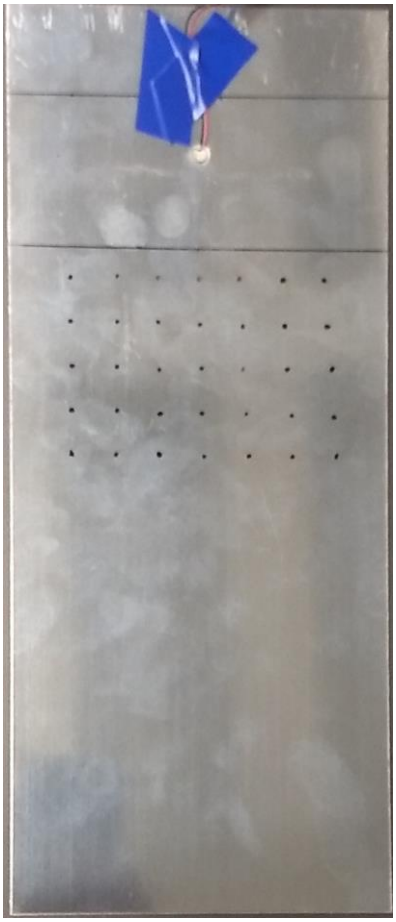

Figure 3- Aluminum Sample

An aluminum sample of $240\,mm \times 140\,mm$ dimensions was used. A piezo electric semsor was attached at a distance of $70\,mm$ from the top of the sample. The sample was clamped on the top and the laser head was placed at a distant of $500\,mm$ from the sample and this distance was kept constant. A total of 5 tests were performed in this investigation.

2.2.1 Parametric Test

The laser has 3 main parameters which effect the functioning of the laser and whether or not the signal would be detected by the piezoelectric sensor. These parameters are the

power supplied to for the laser generation, the pulse duration of the laser and the pulse repetition rate of the laser. The power is measured in percentage of the maximum power, pulse duration (PD) in nanoseconds and the pulse repetition (PRR) rate in kHz. A test was performed to determine the best combination of these three parameters which was used for the other three parameters.

2.2.2 Effect of Added Mass on Propagation of Wave

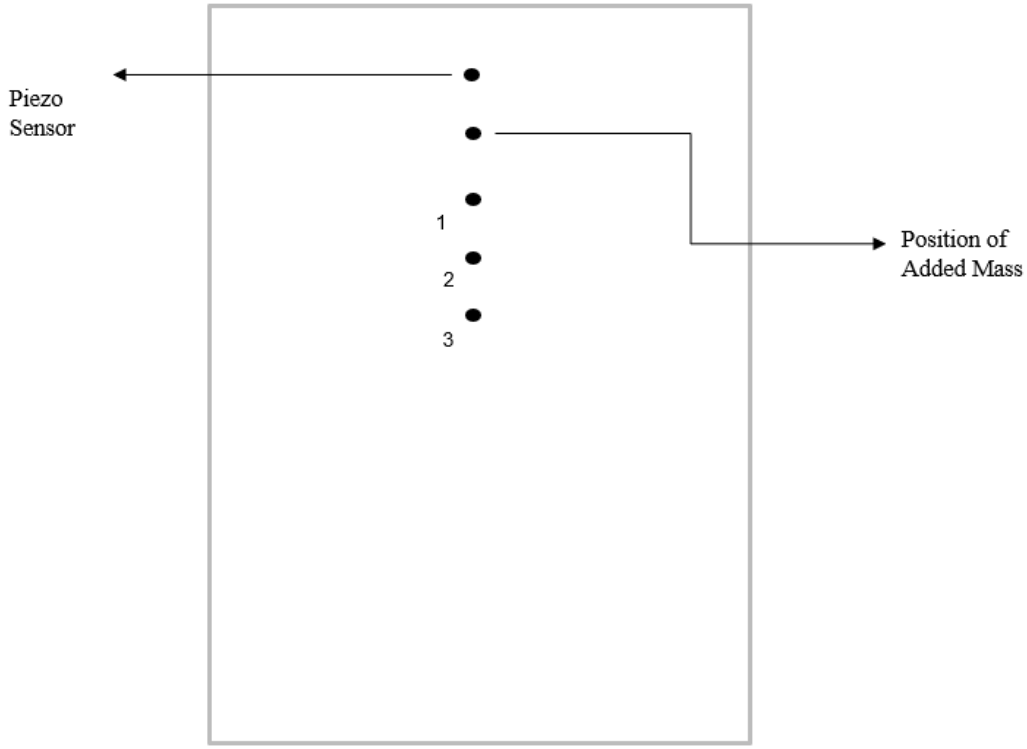

Figure 4 - Path of the laser

In this test, the laser was made to fire at three spots along a vertical path. The spots were at a distance of 40 mm, 55 mm and 75 mm from the Piezo Sensor. The test was performed 5 times and for each iteration of this test, a mass was added in the path between the sensor

and the spots where the laser was fired at a distance of 15 mm from the sensor. The laser parameters for this test were set as 90% Power, 200 ns PD and 60 kHz PRR

2.2.3 Scan of Surface with no added magnets

In this test, the laser and scanner system are used in such a manner so as to perform a raster scan of a certain area of the sample. For the same, the laser is fired at 35 different positions on the sample as is represented by the black spots on the sample itself. These different positions are equidistant from each other (15 mm) in both the X and the Y directions.

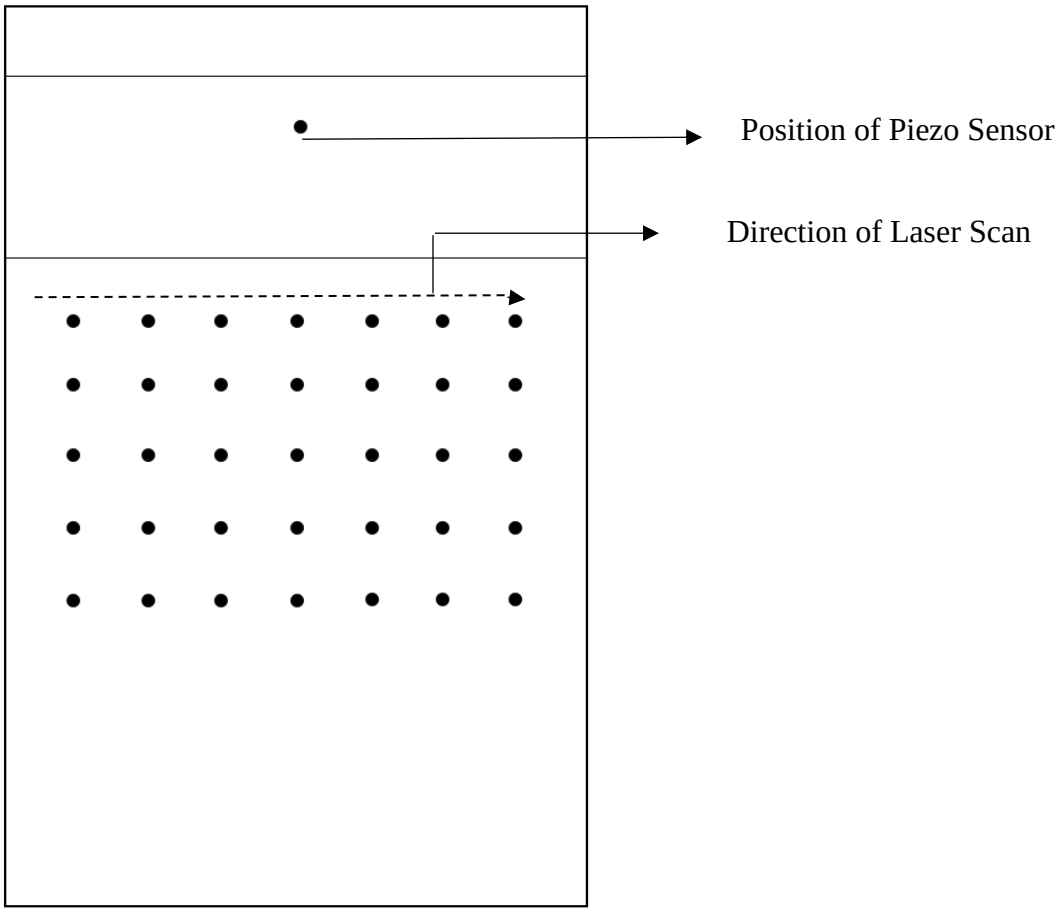

Figure 5 - Position of the points where the laser would be fired for scanning

A regression analysis using the data from this test was also performed to approximate and compare the value of the wave speed.

2.2.4 Scan of surface with added magnets to approximate damage

For this test, magnets were added to the testing sample at random places and the surface of the sample was scanned again. The data collected was used to approximate a damage map.

Figure 6 - The position of the added masses has been indicated in this picture. The additional masses are added at the back of the sample

The image shown above just shows the position where the masses were added on to the sample. While testing, the magnets were not present in between the laser and the sample.

2.2.5 Scan of surface with added mass in between the scanning matrix

The final test was performed with the masses added between the scanning matrix.

Figure 7The position of the added masses has been indicated in this picture. The additional masses are added at the back of the sample

2.2.6 Dense scan of surface with added mass

The final test was performed for a surface with a dense scanning matrix. The scan points were spaced 7.5 mm apart and numbered 117 in total.

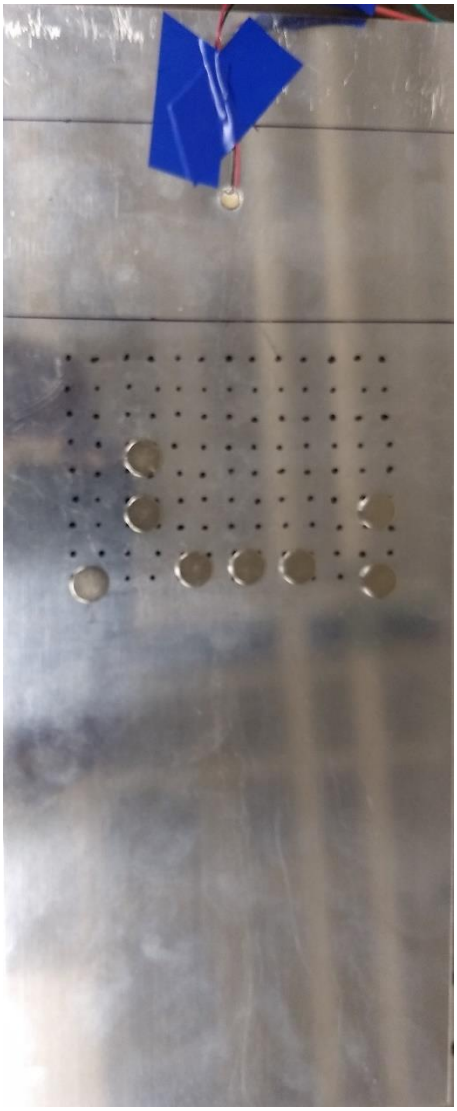

Figure 8The position of the added masses has been indicated in this picture. The additional masses are added at the back of the sample

2.3 Difficulties in Testing

The testing procedure had a few challenges, some of them being of import –

- The selection of proper parameters for the laser testing was challenging and thus necessitated a parametric study of the laser parameters.
- Inclusion of the scanner system was troublesome as there was no optimal way to holster the laser head onto the xy stages without damaging either in the process. A makeshift holster needed to be created to combine both the individual systems together to form a laser scanning system.

CHAPTER 3

DATA PROCESSING AND RESULTS

In this section the procedure behind the processing of the raw data as well as the results of the aforementioned tests would be discussed. For this project, the time of arrival of the wave was chosen as the parameter for differentiating between damaged and normal points as there was no significant change observed in the frequency and the amplitude changes were difficult to quantify as compared to time of arrival which was easily determined.

3.1 Data processing

The data received from the Piezo sensor is inherently noisy and it is tough to discern the origin of the signal to determine the time of flight. The first step in post processing takes place in the oscilloscope itself where the data is filtered with the help of a High Pass filter (140 kHz). This filtration reduces the noise levels to a level which is then manageable with the help of post processing applications like MATLAB's signal processing toolbox

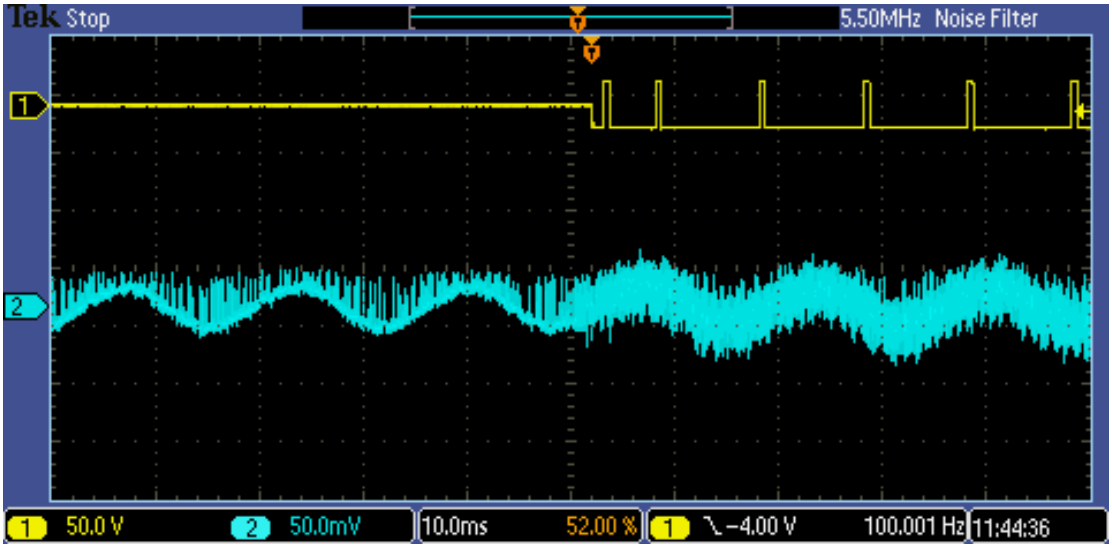

Figure 9 - Data without any Filtering

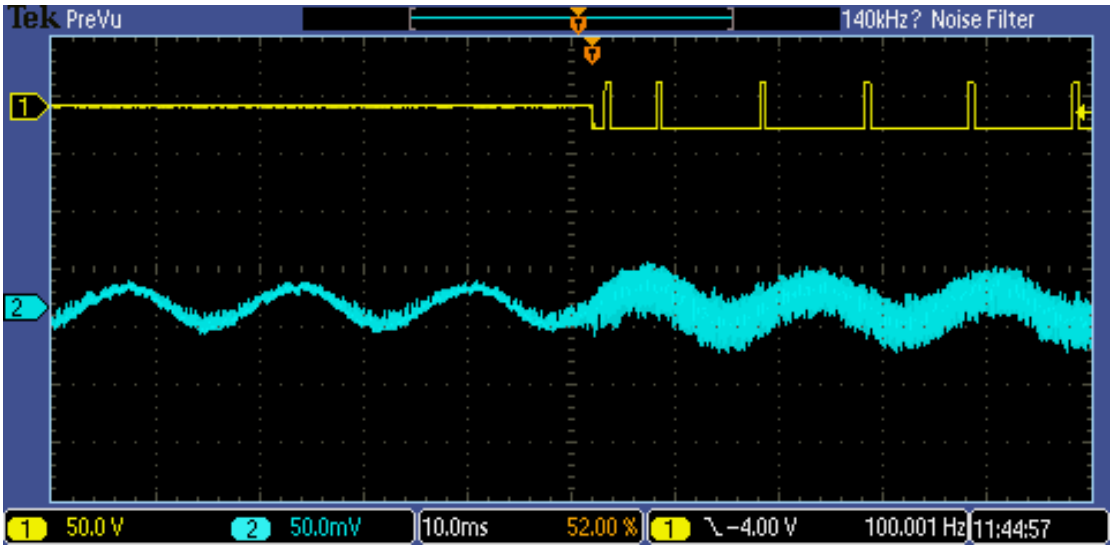

Figure 10 Data after filtering in the oscilloscope

The data after being filtered from oscilloscope is stored in a flash drive and then processed on a remote computer. It is first filtered with the help of a Butterworth Bandpass filter and then an empirical mode decomposition is performed along with a Hilbert Spectral analysis to determine the origin of the signal. This entire process is also called the Hilbert-Huang transform.

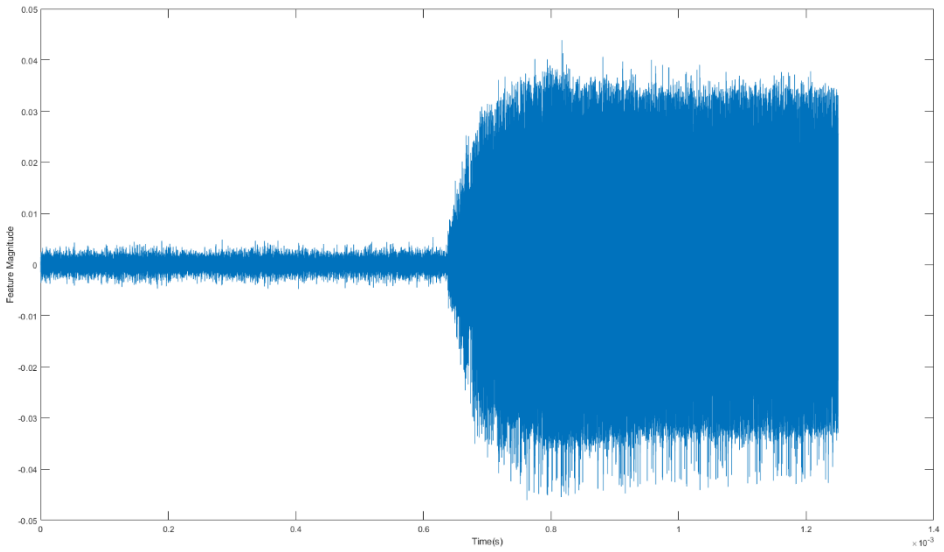

Figure 11 Signal data after Empirical Modal Decomposition

As can be seen, after the post processing we can easily determine the origin of the signal. This time difference is used to determine the time of arrival of the signal.

3.2 Results

The results of all the tests are covered in their own section. After the data was processed it was tabulated for all the spots as well plotted with respect to the corresponding distance from the Piezo Sensor

3.2.1 Parametric Test

For the parametric study, the laser was fired at a spot which was at a distance of 100 mm from the laser the variation of the Laser Power had very little effect on the received signal. As long as the power was above 90%, the signal was clearly received. The laser can only operate at eight specific Pulse Duration values that is, 4ns, 8ns, 14ns, 20ns, 30ns, 50ns, 100ns, 200ns. These values can be selected both from the laser device application as well as by sending commands to the laser using the serial port. Four sets of pulse repetition rate values were chosen for the parametric test; < 20 kHz, 20 kHz to 60 kHz, 60 kHz to 100 kHz and 100 kHz to 140 kHz. The following table shows the parametric study for the influence of the pulse duration and pulse repetition rate on the laser signal.

Pulse Duration / Pulse Repetition Rate	4 ns	8 ns	14 ns	20 ns	30 ns	50 ns	100 ns	200 ns
<20 kHz	○	○	○	○	○	○	●	●
20 kHz to 60 kHz	○	○	○	○	○	○	●	●
60 kHz to 100 kHz	○	○	○	○	○	○	●	●
100 kHz to 140 kHz	○	○	○	○	○	○	○	○
Notes	○ No signal Received ● Faint Signal Received ● Strong Signal Received							

Table 1- Results of the parametric Test

From the table, we can see that the clearest signal was obtained when the pulse duration was 200 ns and pulse repetition rate was < 20 kHz and was thus chosen for testing purposes in general. 200 ns pulse duration and 60 kHz also gave a signal which was observable and thus was used as the parameter for the test 3 only.

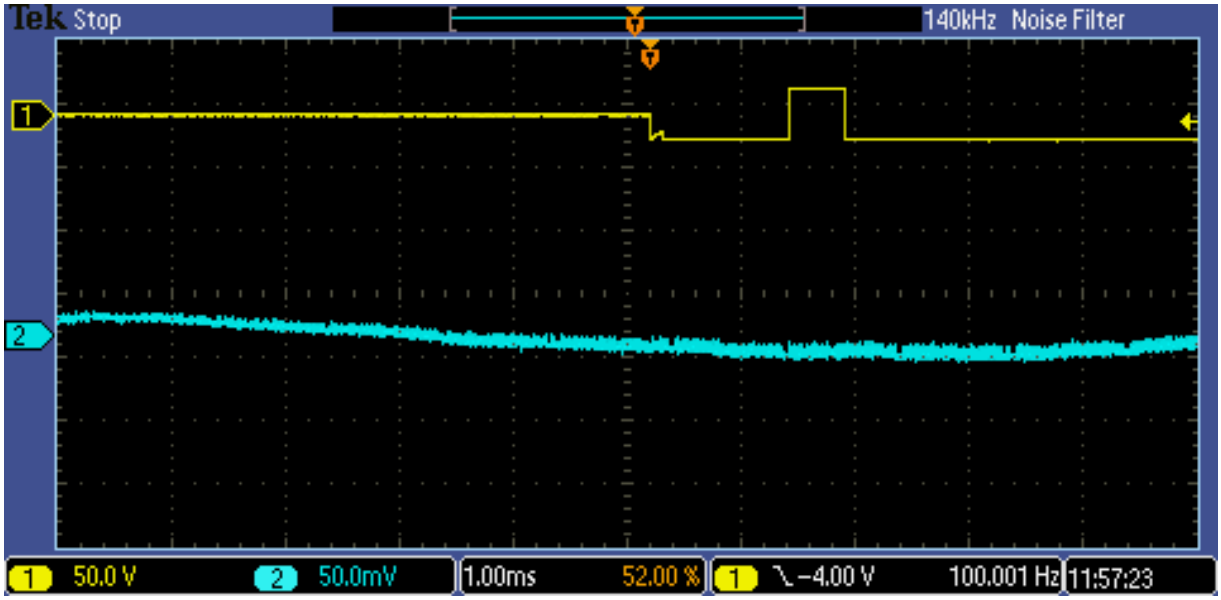

Figure 12 - No signal Received

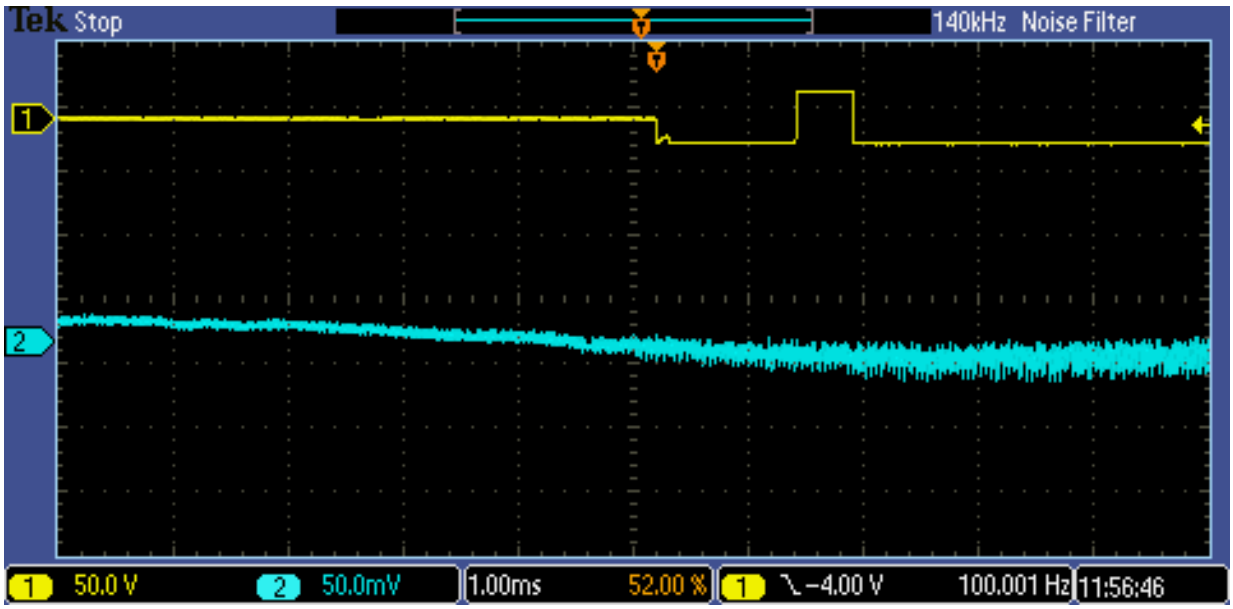

Figure 13- Signal Barely Received

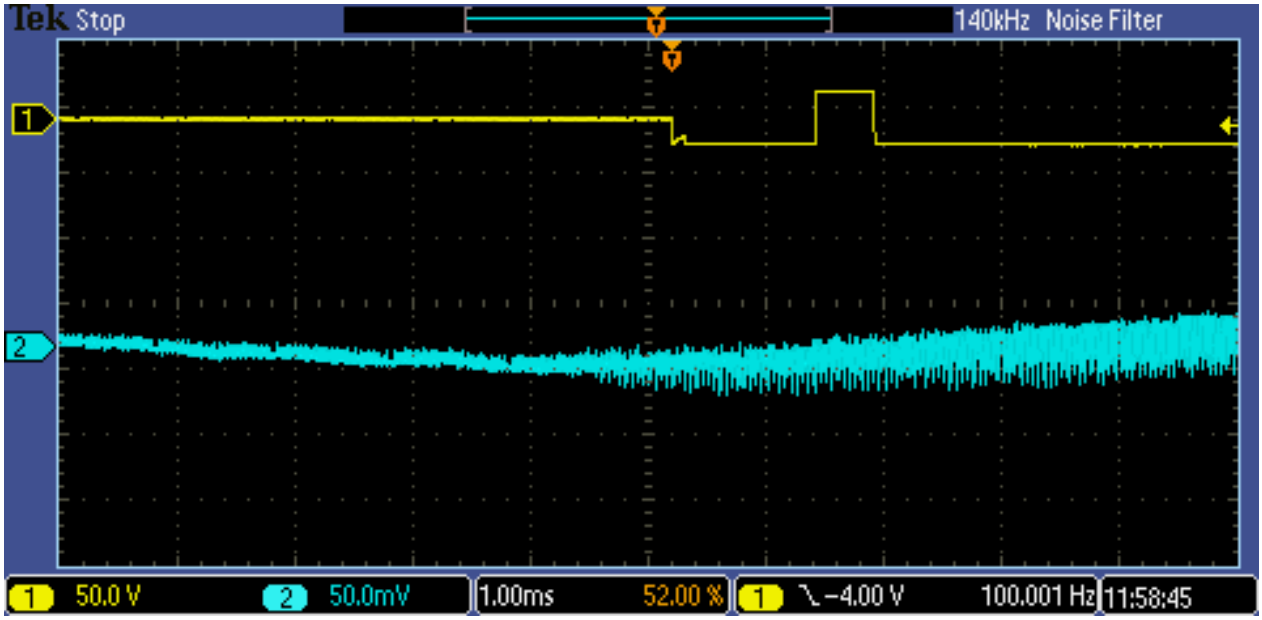

Figure 14 - Signal is clearly Received

3.2.2 Effect of Added Mass on Propagation of Wave

As mentioned before, this test was performed 5 times and for each iteration, a magnet was added to simulate the increment in mass. As is expected, the time of arrival of the wave increases as the distance between the Piezo sensor and the position of contact of the incident laser beam increases. The results, that is the time of arrival in seconds has been documented in table 2 below. The first row represents the three positions of the vertical track the laser beam is fired along and the first column represents the number of added masses.

	1	2	3
1	0.000602	0.0006241	0.000673
2	0.0006101	0.000631	0.0006405
3	0.0006162	0.000634	0.0006411
4	0.0006232	0.000638	0.0006421
5	0.000628	0.00064	0.0006453

Table 2 - Results of Test 2

As we can see, the time of arrival with respect to added masses follows an increasing trend implying that if we have increased distance from the sensor, the speed of the wave would in turn decrease. It is also observed that if we add masses between the laser's incidence point and the piezo sensor, the speed of the sound wave decreases as is shown by an increase in the time of arrival

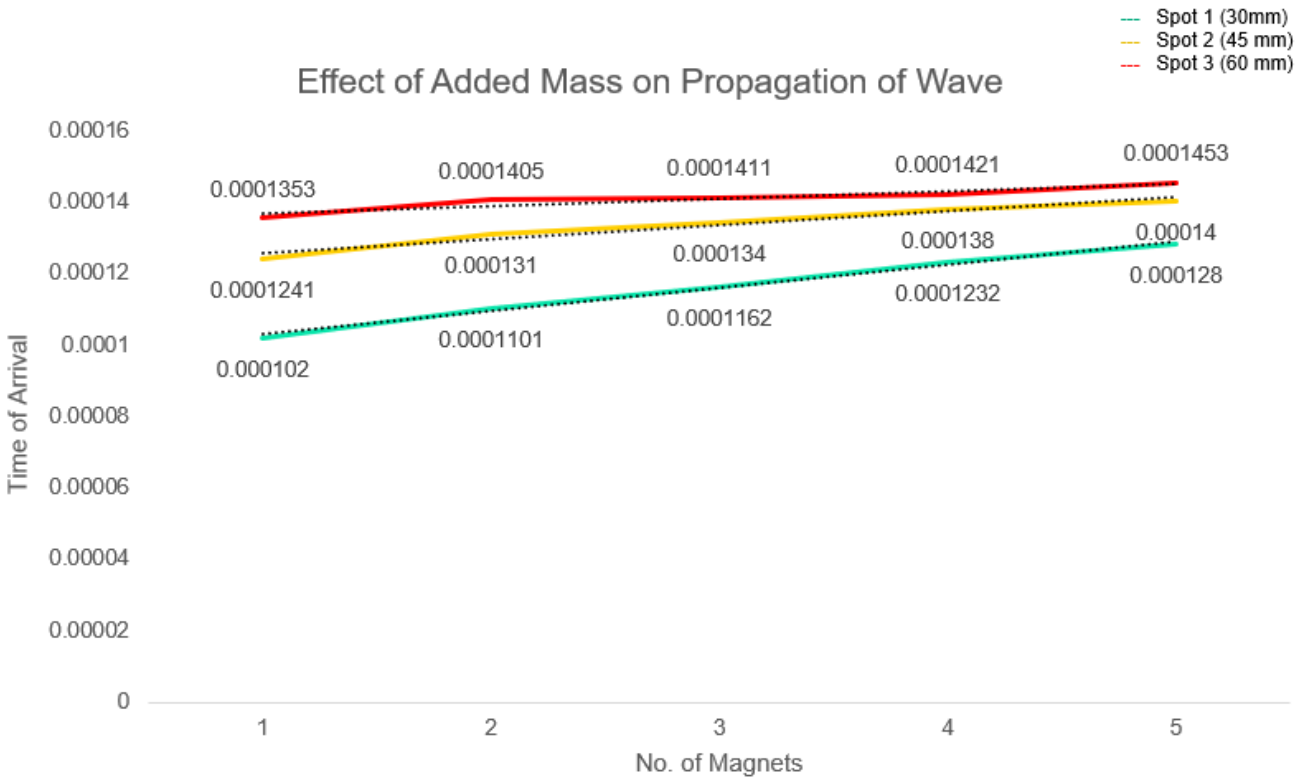

Figure 15Plot of No. of Magnets v/s TOF

The plot above shows how the time of arrival varies as the number of added masses is increased. As can be seen, we see a steady increasing trend of time of arrival as the number of magnets increases.

3.2.3 Scan of surface with no added magnets

The surface selected for testing was also scanned before any damage in the form of magnets was added to the surface. This was done for two reasons –

- Firstly, to compare it to the data which would be derived from the sample after testing it with added masses.
- Secondly, the data is used to perform a regression to determine the calculated value of wave speed to compare with the theoretical value.

Time of arrival(s)	Col. 1	Col. 2	Col. 3	Col. 4	Col. 5	Col. 6	Col. 7
Row 1	0.0000115	0.0000101	0.0000130	0.0000142	0.0000145	0.0000121	0.0000128
Row 2	0.0000149	0.0000135	0.0000133	0.0000128	0.0000120	0.0000117	0.0000144
Row 3	0.0000118	0.0000127	0.0000126	0.0000123	0.0000122	0.0000133	0.0000138
Row 4	0.0000121	0.0000125	0.0000153	0.0000136	0.0000141	0.0000133	0.0000134
Row 5	0.0000151	0.0000141	0.0000136	0.0000119	0.0000123	0.0000149	0.0000132

Table 3- Time of Arrival data for Test 3

As we can see, there is an increase in the time of arrival as the distance from the Piezo Sensor increases.

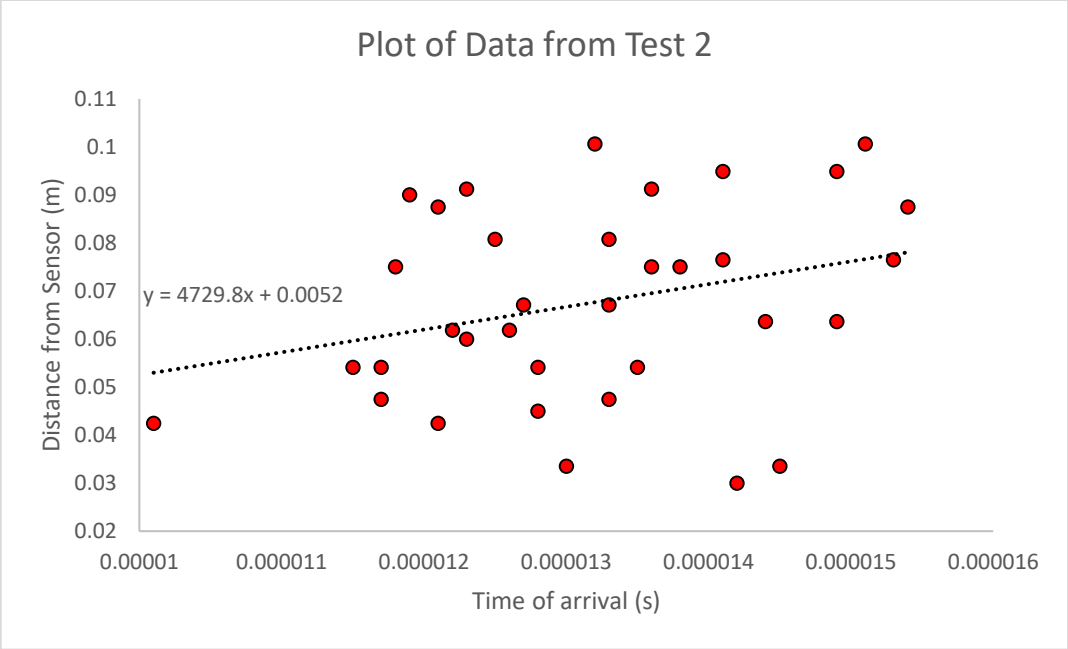

Figure 16Plot of Time of Arrival v/s Distance from Sensor

The data from the second test was plotted with the Time of arrival on the x axis and the Distance from the sensor as the y axis and the regression analysis was performed. The equation shown in the graph is the trend line of the form of $y = a\,x - b$. The wave speed is the coefficient of x in this equation and comes out to be $4729.8\,m/s$. The speed of the wave can be calculated theoretically with the help of the Young's modulus and density –

$$speed\ of\ wave = \sqrt{\frac{E}{\rho}}$$

Where, $E_{aluminium} = 69\ Gpa$ and, $\rho = 2720\ kg/m^3$

Therefore,

$$speed\ of\ wave = 5036.63\ m/s$$

As we can see, our experimental setup gauges the time of arrival properly as is evidenced by the closeness of the experimental and theoretical wave speed values.

3.2.4 Scan of surface with added magnets to approximate damage.

Time of arrival(s)	Col. 1	Col. 2	Col. 3	Col. 4	Col. 5	Col. 6	Col. 7
Row 1	0.0000139	0.0000109	0.0000127	0.0000131	0.0000114	0.0000121	0.0000131
Row 2	0.0000136	0.0000128	0.0000123	0.0000136	0.0000125	0.0000134	0.0000129
Row 3	0.0000132	0.0000125	0.0000126	**0.0000152**	0.0000128	0.0000129	0.0000135
Row 4	0.0000129	0.0000128	0.0000133	**0.0000159**	0.0000131	0.0000126	**0.0000146**
Row 5	**0.0000145**	0.0000135	**0.0000157**	0.0000139	**0.0000151**	0.0000141	**0.0000161**

Table 4- Time of Arrival for data for test 4

The largest ToF is 0.0000161 seconds in row 5 column 6 and the smallest TOF is at row 1 column 6 at 0.0000121 seconds. The average ToF for undamaged area is 0.00001291 seconds and the average ToF for the damaged area is 0.0000153 seconds. The average for the entire area which is scanned is 0.000013408 seconds.

In order to quantify the uncertainty in measurement for the data and the detection probabilities, a bound error of 5% is used as a criterion for determining the which points would be considered damaged and which undamaged by comparing the lower and upper bounds to the time of arrival individually.

The upper and lower bounds were calculated as –

$$Lower\ Bound = Avg - Avg \times 5\%$$

$$Upper\ Bound = Avg + Avg \times 5\%$$

Thus, the criteria are –

$$\text{If } \begin{cases} Lower\ Bound < ToF < Upper\ Bound & \text{Undamaged} \\ ToF < Lower\ Bound\ or\ Upper\ Bound < Tof & \text{Damaged} \end{cases}$$

After this calculation, the lower bound and upper bound were –

$$Lower\ Bound = 0.00001273\ seconds$$

$$Upper\ Bound = 0.00001407\ seconds$$

Thus, we can easily identify the damaged points from Table 4. They are the bolded data points which aligns with the presence of the added masses as well.

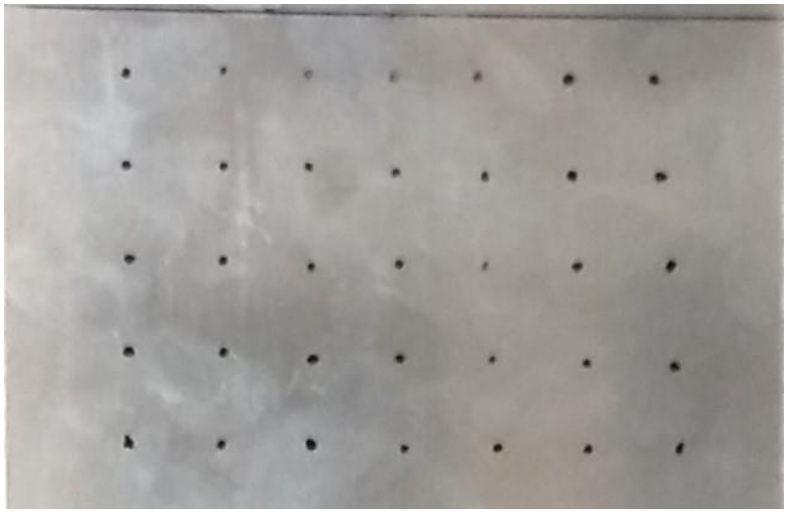

Figure 17 Testing Area

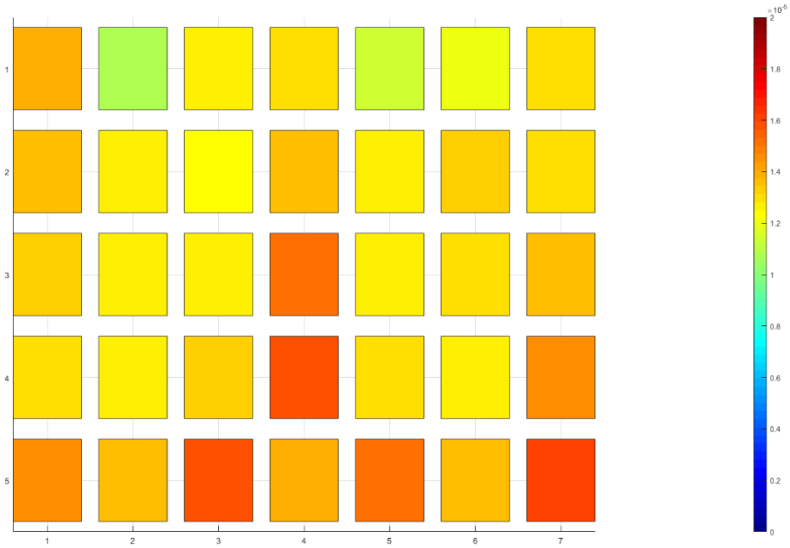

Figure 18 Plot of Tof with respect to relative position of each point

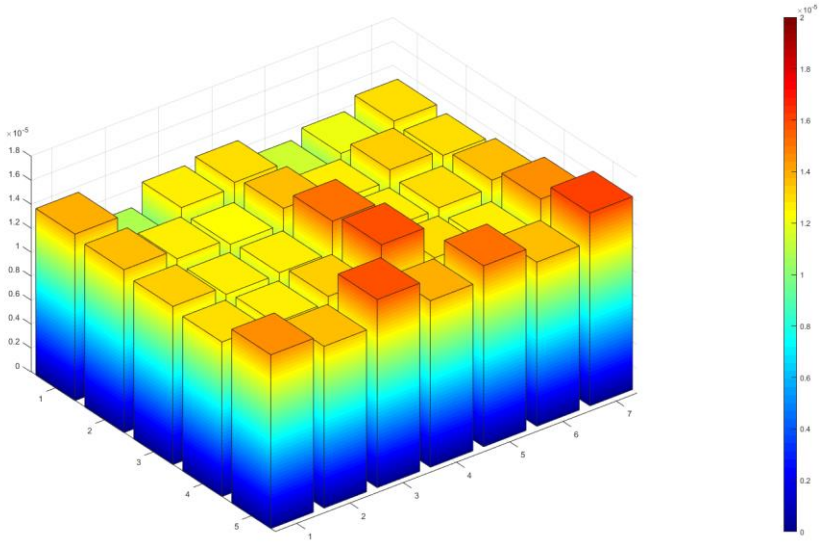

Figure 19 Isometric view of the previous plot

The figures shown above represent a visualization of how the ToF varies along the area of the scanned sample. The points which have damage have a brown-red color and the undamaged points have a blue-green representation. The isometric view is a representation of the changing gradient for the time of arrival between the different spots.

3.2.5 an of surface with added mass in between the scanning matrix

This test was performed to check if the presence of added between the matrix points for scanning would have any effect on the ToF of the points surrounding it.

Time of arrival (s)	Col. 1	Col. 2	Col. 3	Col. 4	Col. 5	Col. 6	Col. 7
Row 1	0.0000 136	0.0000 136	0.0000 132	0.0000 135	0.0000 132	0.0000 106	0.0000 126
Row 2	0.0000 126	0.0000 126	0.0000 107	0.0000 121	0.0000 130	0.0000 123	0.0000 134
Row 3	0.0000 109	0.0000 124	0.0000 133	0.0000 131	0.0000 117	0.0000 138	0.0000 114
Row 4	0.0000 132	0.0000 128	0.0000 113	0.0000 119	0.0000 118	0.0000 113	0.0000 135
Row 5	0.0000 112	**0.0000 140**	0.0000 129	0.0000 111	0.0000 103	**0.0000 141**	0.0000 138

Table 5 Time of Arrival data for Test 5

A similar criterion as the previous test was used to determine the damaged region. The bound values determined were –

$Lower\ Bound = 0.00001124\ seconds$

$Upper\ Bound = 0.0000139\ seconds$

This shows that the spots which are damaged or are near damage are just two. This can be explained by the fact that the points have the closer in proximity to the added mass as

compared to the other points and thus the time of arrival for these points is directly influenced because of their presence.

3.2.6 Dense scan of Surface

The data from the dense scan has been tabulated in the Appendix.

The data from this test was significant in number and thus a Gaussian distribution was fit to the data with the help of MATLAB to develop a criterion for determining the defective points with the help of their ToF. The distribution thus determined had,

$$\mu = 1.34 \times 10^{-5} \quad \& \quad \sigma = 1.28 \times 10^{-6}$$

Since the test involves masses being added to simulate damage, implying that the density at that point would be higher, the ToF for a defective point thus would be higher than the general ToF. Thus, the criteria was that if the values lie in the cumulative probabilities for positive z-values for a certain confidence level, they would be non-defective. The confidence levels chosen were 95%, 90%, 85%, 80% and 75%.

According to the scanned region, a total of 24 points should have been identified as defective. The different confidence levels were able to determine the points with defective ToF with varying success.

Confidence Level	Defective points detected
95%	4
90%	7
85%	15
80%	20
75%	24

Table 6 Points Detected by the different Criterion

Thus, we are able to determine all the points by the 75% confidence level. If the defects were of a kind wherein the density effectively reduces, then the ToF would be lower than the general TOF. Thus, the negative z-values can be used for determining the defective points in that case.

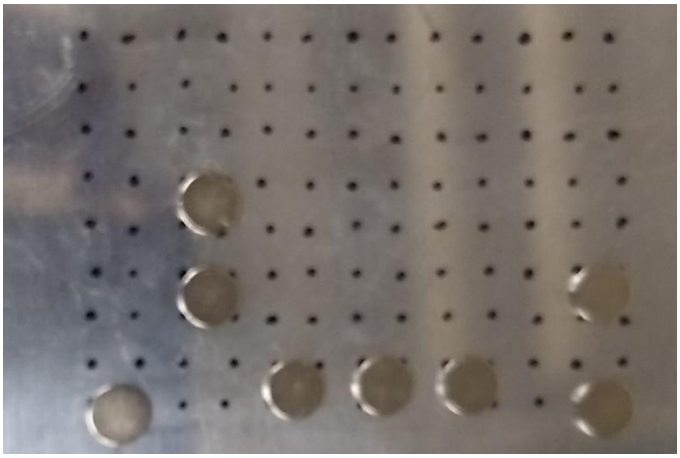

Figure 20Location of added masses for dense Scan

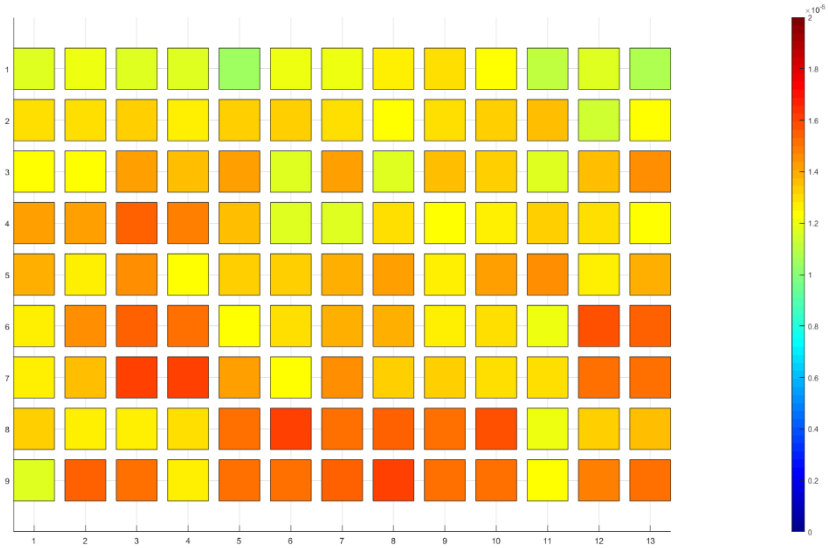

Figure 21Dense Scan Top view of ToF

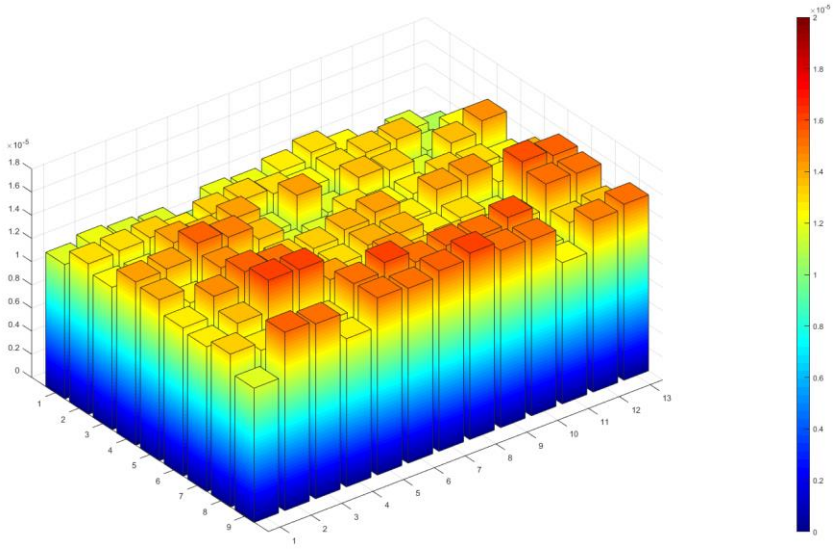

Figure 22Dense Scan ToF Isometric View of Plot

CHAPTER 4

CONCLUSION AND FUTURE WORK

Laser scanning technology is a widely used method for damage detection and has extremely varied applications. It is a valuable technique as it is a non-destructive technique which is not only cheap but in most cases is easy to setup and use.

This research focused on developing a novel method for using laser induced ultrasonic waves for non-destructive testing. To that end first a scanning system needed to be developed so that the laser could moved on the surface of a test sample. This was achieved by holstering the laser head onto an ASI xy stage which was then controlled by a computer. Once the scanner system was developed, a series of tests were performed on the sample. The first was a parametric test which was used to decide the operational parameters of the laser. The next test was done to determine the effect of added mass on the laser induced ultrasound and it was found that as the number of added masses increased, so did the time of arrival.

To establish that the time of arrival determined by this laser scanning method was indeed logical and the wave speed thus determined would resemble the theoretical values which can be calculated, the third test involved scanning the surface of the sample to determine an approximate of the wave speed. This data was then plotted with respect to the distance from the piezoelectric sensor and a linear regression was performed to determine the speed of the ultrasound wave. The speed of the wave determined in such a fashion was found to be close to the value which can be calculated theoretically.

The fourth test was a scan of the surface after masses were added to the sample's surface to visualize damage. The data from this test was plotted and a criterion was determined to estimate the points which had damage. The damaged points determined from this criterion was a perfect match to the damaged points actually present. Thus, this method was found to be able to determine whether or not a point is damaged if the laser is fired on that specific point. The fifth test's purpose was to determine if the time of arrival would be affected if the added mass in between the scanning matrix. A similar criterion as test four was used in this test as well to find the damaged points. The criteria however only found two points to be damaged leading to the conclusion that unless the damaged region is in close proximity or in the path of the incidence of the laser beam, the time of arrival would not be affected.

For the final test, the scanning matrix was made denser so as to increase the number of scanning points and masses were added to simulate damage. As the number of points scanned in this test was more, a Normal distribution was fit to this data with the help of MATLAB. As mass is only added to the surface, it was assumed that any ToF which is significantly higher would be defective. Thus, the data in the positive confidence limit was assumed to be non-defective and higher than that was defective. It was found that 80% confidence was able to detect the most defective points easily.

In future, the entire scanning system can be improved so that more minute movements of the laser is possible so as to improve the resolution of the scan. The scanning system also needs to be made more robust so that the scanning of a larger area of the sample is possible.

The regression study performed in test 3 for the wave speed was only performed for 35 points. The sample size an be increased for a more accurate value of the wave speed. In this study, the test number 4 was only performed with a single added mass on each of the damaged points. For future testing the effect of the increase in the number of added masses on the time of arrival is something which needs to be studied.

REFERENCES

1. Ihn, J., & Chang, F. (2004). Detection and monitoring of hidden fatigue crack growth using a built-in piezoelectric sensor/actuator network: II. Validation using riveted joints and repair patches. *Smart Materials and Structures, 13*(3), 621-630. doi:10.1088/0964-1726/13/3/021

2. Harb, M., & Yuan, F. (2015). A rapid, fully non-contact, hybrid system for generating Lamb wave dispersion curves. *Ultrasonics, 61*, 62-70. doi:10.1016/j.ultras.2015.03.006

3. Huang, N. E. (n.d.). An Adaptive Data Analysis Method for Nonlinear and Nonstationary Time Series: The Empirical Mode Decomposition and Hilbert Spectral Analysis. *Wavelet Analysis and Applications Applied and Numerical Harmonic Analysis*, 363-376. doi:10.1007/978-3-7643-7778-6_25

4. K. Dragan, M. Dziendzikowski, T. Uhl, and L. Ambrozinski, "Damage detection in the aircraft structure with the use of integrated sensors - SYMOST project," *Proc. 6th Eur. Work. - Struct. Heal. Monit. 2012, EWSHM 2012*, vol. 2, pp. 974–980, 2012

5. W. Ostachowicz, T. Wandowski, and P. Malinowski, "Damage Detection Using Laser Vibrometry," *NDT Aerosp.*, pp. 1–8, 2010.

6. M. Ochiai, "Development and Applications of Laser-ultrasonic Testing in Nuclear Industry," *Int. Symp. Laser Ultrason. Sci. Technol. Appl.*, vol. Science, T, no. March, pp. 4–12, 2008.

7. L. Mallet, B. C. Lee, W. J. Staszewski, and F. Scarpa, "Structural health monitoring using scanning laser vibrometry: II. Lamb waves for damage detection," *Smart Mater. Struct.*, vol. 13, no. 2, pp. 261–269, 2004.

8. S. E. Burrows, S. Dixon, S. G. Pickering, T. Li, and D. P. Almond, "Thermographic detection of surface breaking defects using a scanning laser source," *NDT E Int.*, vol. 44, no. 7, pp. 589–596, 2011.

9. Yantchev, V., & Katardjiev, I. (2013). Thin film Lamb wave resonators in frequency control and sensing applications: A review. *Journal of Micromechanics and Microengineering, 23*(4), 043001. doi:10.1088/0960-1317/23/4/043001

10. Kessler, S. S., Spearing, S. M., & Soutis, C. (2002). Damage detection in composite materials using Lamb wave methods. *Smart Materials and Structures, 11*(2), 269-278. doi:10.1088/0964-1726/11/2/310

APPENDIX A

TOF DATA FOR TEST 6

	Column 1	Column 2	Column 3	Column 4
Row 1	0.0000116	0.0000121	0.0000118	0.0000116
Row 2	0.000013	0.0000131	0.0000132	0.0000125
Row 3	0.0000123	0.0000123	0.0000141	0.0000136
Row 4	0.0000141	0.0000142	0.0000154	0.0000149
Row 5	0.0000139	0.0000126	0.0000146	0.0000123
Row 6	0.0000128	0.0000145	**0.0000156**	**0.0000151**
Row 7	0.0000125	0.0000135	**0.0000162**	**0.0000144**
Row 8	0.0000132	0.0000125	0.0000126	0.0000129
Row 9	**0.0000148**	**0.0000154**	0.0000131	0.0000128

	Column 5	Column 6	Column 7	Column 8
Row 1	0.0000104	0.0000121	0.0000119	0.0000125
Row 2	0.0000132	0.0000134	0.0000129	0.0000123
Row 3	0.0000142	0.0000118	0.0000141	0.0000116
Row 4	0.0000137	0.0000117	0.0000118	0.0000131
Row 5	0.0000132	0.0000132	0.0000138	0.0000143
Row 6	0.0000122	0.0000131	0.0000138	0.0000138
Row 7	0.0000142	0.0000124	0.0000144	0.0000132
Row 8	**0.0000152**	**0.000016**	**0.000015**	**0.0000154**
Row 9	**0.0000153**	**0.0000151**	**0.0000156**	**0.0000161**

	Column 9	Column 10	Column 11	Column 12	Column 13
Row 1	0.0000131	0.0000122	0.0000111	0.0000118	0.0000107
Row 2	0.0000129	0.0000134	0.0000135	0.0000115	0.0000123
Row 3	0.0000136	0.0000132	0.0000117	0.0000135	0.0000144
Row 4	0.0000123	0.0000125	0.0000132	0.0000129	0.0000123
Row 5	0.0000126	0.0000142	0.0000144	0.0000128	0.0000138
Row 6	0.0000127	0.0000131	0.0000121	**0.0000159**	**0.0000154**
Row 7	0.0000134	0.0000129	0.0000131	**0.0000153**	**0.0000147**
Row 8	**0.0000152**	**0.0000158**	0.0000121	0.0000133	0.0000136
Row 9	**0.0000153**	**0.0000152**	0.0000122	**0.0000148**	**0.0000152**

The column and row numbers correspond to the scan point on the scanning matrix. The points bolded represent the points with the defects as the TOF there is higher than the 75% confidence limit.

APPENDIX B

MATLAB COMMANDS UTILIZED

Three major MATLAB commands were used in this project.

- The first is emd which is used to perform the empirical modal decomposition of the signal data to determine the ToF.

- The second major command was the $fitdist$ command to fit the Gaussian distribution to the data from test 6.

- The last major command is the $bar3$ command used for the 3d plots.